Published in final edited form as:
Neurobiol Dis. 2013 January ; 0: 200–210. doi:10.1016/j.nbd.2012.07.019.

Limited regional cerebellar dysfunction induces focal dystonia in mice

Robert S. Raike[1], **Carolyn E. Pizoli**[4,*], **Catherine Weisz**[4,5,*], **Arn M. J.M. van den Maagdenberg**[6], **H.A. Jinnah**[2,3], and **Ellen J. Hess**[1,2,†]

[1]Department of Pharmacology, Emory University School of Medicine, Atlanta, GA 30322 [2]Department of Neurology, Emory University School of Medicine, Atlanta, GA 30322 [3]Department of Human Genetics, Emory University School of Medicine, Atlanta, GA 30322 [4]Department of Neurology, Johns Hopkins University School of Medicine Baltimore, MD 21287 [5]Department of Neuroscience, Johns Hopkins University School of Medicine Johns Hopkins, Baltimore, MD 21287 [6]Departments of Human Genetics and Neurology, Leiden University Medical Centre, 2300 RC Leiden, The Netherlands

Abstract

Dystonia is a complex neurological syndrome broadly characterized by involuntary twisting movements and abnormal postures. The anatomical distribution of the motor symptoms varies among dystonia patients and can range from focal, involving an isolated part of the body, to generalized, involving many body parts. Functional imaging studies of both focal and generalized dystonia in humans often implicate the cerebellum suggesting that similar pathological processes may underlie both. To test this, we exploited tools developed in mice to generate animals with gradients of cerebellar dysfunction. By using conditional genetics to regionally limit cerebellar dysfunction, we found that abnormalities restricted to Purkinje cells were sufficient to cause dystonia. In fact, the extent of cerebellar dysfunction determined the extent of abnormal movements. Dysfunction of the entire cerebellum caused abnormal postures of many body parts, resembling generalized dystonia. More limited regions of dysfunction that were created by electrical stimulation or conditional genetic manipulations produced abnormal movements in an isolated body part, resembling focal dystonia. Overall, these results suggest that focal and generalized dystonias may arise through similar mechanisms and therefore may be approached with similar therapeutic strategies.

[†]Address correspondence to: Ellen J. Hess, Ph.D., Departments of Pharmacology and Neurology, Emory University School of Medicine, 101 Woodruff Circle, WMB 6303, Atlanta, GA 30322, Phone: 404-727-4911, Fax: 404-712-8576, eyhess@emory.edu.
[*]Current address (for CEP) Division of Pediatric Neurology, Duke University Medical Center, Durham, NC, 27710 and (for CW) Department of Otolaryngology, University of Pittsburgh School of Medicine, Pittsburgh, PA, 15261

Keywords

Focal dystonia; cerebellum; lentivirus; electrical stimulation; cre recombinase

Introduction

Dystonia is characterized by involuntary muscle contractions that give rise to twisting movements and abnormal postures. The anatomical distribution of the dystonic movements varies considerably among affected individuals. Focal dystonias, such as writer's cramp or torticollis, affect one part of the body, whereas generalized dystonia encompasses much of the body. The relationship, if any, between focal and generalized dystonia is not understood. However, some evidence suggests that focal and generalized dystonias reflect different extents of the same underlying pathobiology since focal dystonias sometimes evolve into generalized dystonia (Bressman et al., 2009; Camargos et al., 2008; Kamm, 2006; Nemeth, 2002). Further, within families affected by dystonia-causing gene mutations, some members suffer from generalized dystonia whereas others exhibit focal dystonias (Kamm, 2006; Nemeth, 2002), suggesting that a spectrum of dystonias can arise from similar pathologic processes.

Because most dystonias results from dysfunction, rather than overt degeneration, functional imaging in patients is frequently used to localize abnormal brain activity. These studies often reveal abnormalities in basal ganglia and cortex. Imaging studies also frequently reveal involvement of the cerebellum (Neychev et al., 2011; Zoons et al.). Diffusion tensor imaging in dystonia patients implicates abnormal cerebellothalamic connectivity (Argyelan et al., 2009). Abnormal cerebellar activity is observed with PET and fMRI imaging in generalized and segmental dystonias, including DYT1 dystonia (Eidelberg et al., 1998), hemidystonia (Ceballos-Baumann et al., 1995), and exercise-induced paroxysmal dystonia (Kluge et al., 1998). Abnormal cerebellar activity is also observed in focal dystonias, including writer's cramp (Odergren et al., 1998; Preibisch et al., 2001), cervical dystonia (Galardi et al., 1996) and blepharospasm (Hutchinson et al., 2000). More specifically, *increases* in cerebellar perfusion or metabolism are consistently observed across functional imaging studies in dystonic patients, regardless of form or etiology. Thus, cerebellar dysfunction is a common feature of focal and generalized dystonias, suggesting that different forms of dystonia share similar pathological processes differing only by the region or amount of cerebellum affected.

While it is challenging to determine the relationship between focal and generalized dystonia from functional imaging in patients, animals can be used to test hypotheses suggested by the results of studies performed in humans. Because there are no widely accepted primate models of dystonia, rodents are generally used for such studies. Similar to the imaging studies in patients, abnormal cerebellar activation is observed in several different genetic rodent models of dystonia, including both transgenic and knockin *DytI* mice, dystonic (*dt*) rats and *tottering* mice (Brown and Lorden, 1989; Calderon et al., 2011; Campbell and Hess, 1998; Ulug et al., 2011; Zhao et al., 2011). Eliminating cerebellar output abolishes generalized dystonia in *dt* rats and *tottering* mice (Campbell et al., 1999; LeDoux et al., 1993). Conversely, abnormal cerebellar activation via AMPA receptor agonists induces

generalized dystonia in normal mice (Fan et al., 2012; Pizoli et al., 2002). The ability to both eliminate and evoke generalized dystonia in rodents through cerebellar manipulations suggests that this approach can be refined to better understand the mechanisms underlying the distribution of the abnormal movements in focal or generalized dystonia. Therefore, we exploited tools developed in mice to determine if similar mechanisms could govern both isolated abnormal movements, such as those observed in focal dystonia and abnormal movements that affect the entire body, such as those observed in generalized dystonia.

Materials and Methods

Mice

Tottering (B6.D2-*Cacna1a*^{tg}/J) mice, *Rosa26* mice (B6.129S4 Gt(ROSA)26Sortm1Sor/J), and *L7-cre* transgenic mice (B6.129-Tg(Pcp2-cre)2Mpin/J) on strain C57BL/6J were obtained from The Jackson Laboratory (Bar Harbor, ME). Transgenic mice expressing the coding region of the SV40 large T antigen driven by the pcp-2/L7 Purkinje cell specific promoter (*L7-Sv4* mice) on strain FVB were kindly provided by Drs. R. Feddersen and H. Orr (University of Minnesota); these mice were outcrossed to C57BL/6J and then backcrossed to C57BL/6J for 5 generations before use. Mice carrying floxed *Cacna1a* alleles (*Cacna1a*$^{flox/flox}$) on strain C57BL/6J were as described (Todorov et al., 2006). Mice carrying a null *Cacna1a* allele (*Cacna1a*$^{+/-}$) on the mixed strain C3H-C57BL/6J were kindly provided by Dr. D. Yue (Johns Hopkins University). Male and female mice were used in all experiments. All mice were bred at Emory University or Johns Hopkins University vivaria, housed on a 12 hr light/dark cycle and had access to food and water *ad libitum*. Experiments were in accordance with the Guide for the Care and Use of Laboratory Animals as adopted by the United States National Institutes of Health, Emory University and Johns Hopkins University.

To genotype mice, PCR was performed using genomic DNA from tail biopsies with forward and reverse primers: for the *Cacna1a*^{tg} allele, 5′-GGAAACCAGAAGCTGAACCA-3′ and 5′-GAAATGGAGGAATTCAGGG-3′; for the *L7-Sv4* transgene, 5′-AGTACTGTCCCCCAAGAGATAGTAG-3′ and 5′-CCATTCATCAGTTCCATAGGTTGG-3′; for the *Cacna1a*^{flox} allele, 5′-ACCTACAGTCTGCCAGGAG-3′ and 5′-TGAAGCCCAGACATCCTTGG-3′; for the *L7-Cre* transgene, 5′-GCGGTCTGGCAGTAAAAACTATC-3′ and 5′-TCTCTGACCAGAGTCATCCTTAGC-3′; for the *Cacna1a* null allele, 5′-ATAATAAGTCACCTCTCGTTCTAAAG-3′ and 5′-CTGACTAGGGGAGGAGTAGAAG-3′; for the *Rosa26* allele, 5′-GCGAAGAGTTTGTCCTCAACC-3′ and 5′-GGAGCGGGAGAAATGGATATG-3′. PCR products for the *Cacna1a*^{tg} allele were sequenced to detect the C1802T mutation.

Assessments of abnormal movements

Behavior was observed and scored for 1 min at 10 min intervals for 60 min. Motor scores were determined by recording the presence or absence of abnormal postures in the 3 different body regions (limbs, trunk, head/neck), making 6 the highest score/region and 18 the highest total motor score/60-min session. No abnormal movements was defined as a total score of ≤ 1. For the *Cacna1a*$^{tg/flox}$; *L7-Cre* (*tottering*$^{PC\text{-}haplo}$) mice, a behavioral inventory was also used to define the type of movements, including tremor (trunk, limbs, neck and head), tonic flexion, extension (trunk, limbs, neck and head) or twisting (trunk and neck),

and clonus (limbs and head); this instrument was previously described and validated in mice (Devanagondi et al., 2007; Shirley et al., 2008). The behavioral inventory also was used in the lentivirus and electrical stimulation experiments. Behavioral inventory scores were calculated by summing all movements over the 60 min session. For electrical stimulation only, scores corresponded to the 10 min interval for each of the stimulation amplitudes. For the prospective study using the *L7-Sv4* transgenic mice, mice were assessed every 3 weeks from 4-25 weeks of *L7-Sv4* age. Fourteen *L7-Sv4* transgenic mice started in the experiment and mice were removed from the study; motor score was assessed for all at week 4 and week 7. Subsequently, about 4 mice were removed from the study within each interval depicted in Figure 1 to determine Purkinje cell counts. Purkinje cells were counted in all mice (see below). Mice injected with lentivirus were assessed weekly for up to 13 weeks and the maximum behavioral inventory score achieved by each mouse was used. All other mice were assessed once. Except for electrical stimulation, abnormal movements were induced by administration of 15 mg/kg caffeine, which triggers generalized dystonia in nearly 100% of *tottering* mice (Fureman et al., 2002). During behavioral assessments, mice were placed individually in clean mouse cages. Experimenters were blinded to genotype or treatment for all experiments except electromyography.

Lentivirus injections

Mice were anesthetized with tribromoethanol (Sigma-Aldrich, St. Louis, MO). Lentivirus constructs encoding either Cre or GFP under the control of the CMV promoter (Maguschak and Ressler, 2008) were generously provided by Dr. K. Ressler. Mice were positioned in a stereotaxic apparatus, a small hole was made in the skull and 1 μl of CMV-Cre or CMV-GFP viral solution at $\sim 10^9$ IFU/ml (Emory University Viral Vector Core, Atlanta, GA) was delivered (-6.5 mm AP from bregma, 0 or 2 mm ML [vermis and paravermis] and 1.5 mm Vert from the skull surface) at a rate of 0.075 μl/min. Motor behavior was assessed beginning 7-10 days after surgery.

Electromyography (EMG)

A 2-channel wireless transmitter (F20-EET, Data Sciences International, St. Paul, MN) was implanted dorsally, leads were threaded underneath the skin to the hindlimb and fine wire electrodes were inserted and secured into the tibialis and gastrocnemius muscles. Wounds were sutured and topically sealed with Nexaband (Veterinary Products Laboratories, Phoenix, AZ). Mice were assessed beginning 24-48 hr after surgery. EMG was recorded telemetrically in awake, freely-moving mice at 500 Hz using PhysioTel cage-bottom receivers and the Dataquest A.R.T. 4.1 software package (Data Sciences International). Raw EMG data was digitally processed using 75/225 Hz high/low-pass Butterworth filters with the Spike2 software package (Cambridge Electronic Design, Cambridge, UK). The root mean square (RMS) was calculated using a 10 ms time constant; data are reported as peak RMS rounded to the nearest 1 μV. To assess normal EMG activity, peak RMS data was calculated from random 1 s epochs during walking. The abnormal hindlimb movements in *tottering* mice were associated with brief 50-350 ms high-amplitude events (mean peak RMS amplitude for TA = 520±132 μV and for GS = 649±130 μV) that signaled the onset of movement. Normal mice also exhibit brief high-amplitude EMG events (mean peak RMS amplitude for TA = 332±88 μV and for GS = 436±226 μV) associated with the onset of

vigorous hindlimb movements such as scratching. Therefore, these high-amplitude events were used as objective markers for data analysis whereby RMSs were calculated from 5 s epochs immediately following high-amplitude events (14-302 samples analyzed/mouse).

Electrical stimulation of the cerebellum

Mice were anesthetized with tribromoethanol (Sigma- Aldrich, St. Louis, MO) and positioned in a stereotaxic apparatus. A bipolar concentric microelectrode with a 0.5 mm shaft and a 0.5 mm active tip 150 μm in diameter (PlasticsOne, Roanoke, VA) was implanted -6.5 mm AP from bregma, 2 mm ML and 1.5 mm Vert from the skull surface and secured with dental acrylic. Cerebellar stimulation was performed in awake, freely-moving normal mice 24-48 hr after surgery using an A310 Accupulser coupled to an A365 stimulus isolator (World Precision Instruments, Sarasota, FL), which delivered 1 s trains of 100 μs biphasic pulses every 4.5 s at a frequency of 500 Hz. The stimulation amplitude was increased from 100 μA to 400 μA in 100 μA increments every 10 min. To preclude potential artifacts from tissue damage, charge density was held between ∼4-16 μC/cm^2/phase throughout the experiment, which is below the United States Food and Drug Administration recommended safety limit of 30 μC/cm^2/phase. After each experiment electrode implantation sites were verified. No evidence of tissues damage was observed.

Histological assesssments

For *in situ* hybridization for calbindin, the entire cerebellum was sectioned in the coronal plane at a thickness of 30 μm. A 1.2 kb fragment of mouse calbindin cDNA (kindly provided by Dr. T.L. Wood, University of Medicine and Dentistry of New Jersey) was used to transcribe a cRNA probe. Transcription and hybridization reactions were performed as described previously (Campbell and Hess, 1998), except digoxigenin RNA labeling and colorimetric detection kits were used according to the manufacturer's guidelines (Roche Diagnostics, Penzberg, Germany). Slides were hybridized with 5-15 ng labeled cRNA probe at 56°C overnight. Sections were counterstained with Nuclear Fast Red (Vector Laboratories, Burlingame, CA). To calculate the linear density of Purkinje cells, each set of cerebellar sections was numbered caudal to rostral and a pseudorandom starting point within the first 7 sections was designated as the first for analysis. Every seventh section afterward was analyzed until the rostral end of cerebellum was reached. Sections were examined under bright-field illumination using an upright BX51 light microscope (Olympus, Center Valley, PA) with a computer-controlled MAC 2000 motorized microscope stage (Ludl Inc, Hawthorne, NY). Purkinje cell layers were traced and calbindin-positive Purkinje cell contours were marked and counted using the Stereoinvestigator/Neurolucida software package (Microbrightfield Inc, Williston, VT). The linear density of Purkinje cells was calculated by dividing the total Purkinje cell count by total Purkinje cell layer length (PC/mm). Using these methods, the total Purkinje cell count in the normal C57BL/6J mouse and *tottering* mouse cerebellum (mean total PC count = 177,192±5,937 for normal and 175,256±9,214 for *tottering*; n = 5 and 12, respectively; $p = 0.9$, determined by Student's *t* test), was consistent with previously reported findings (Hadj-Sahraoui et al., 1997; Heckroth et al., 1989). Representative images were obtained using a Spot Insight digital camera (Diagnostic Instruments, Sterling Heights, MI). For serial reconstructions of the cerebellum, the most caudal section was assigned a Z value of 0 μm and a section thickness of 30 μm.

Successive sections were automatically assigned a Z value based upon the section interval and aligned using the Joy-Free joystick mode of the Stereoinvestigator software package.

For β-galactosidase immunohistochemistry, staining was performed on free-floating sections incubated in β-galactosidase antibody (1:8000; Abcam, Cambridge, MA) for 2 days at 4°C, incubated in the secondary antibody (1:800 dilution) for 1 day at 4°C and developed using the Vectastain Elite ABC kit (Vector Labs, Burlingame, CA). For X-gal staining after intracerebellar injections of CMV-Cre lentivirus, whole brains were fixed in ice-cold 0.25% glutaraldehyde in PBS for 1 hr and incubated overnight at 37°C in 0.02% Igepal (Sigma), 0.01% sodium deoxycholate, 2 mM $MgCl_2$, 5 mM potassium ferricyanide, 5 mM potassium ferrocyanide and 1 mg/ml X-gal in PBS. Brains were post-fixed in 10% buffered formalin at 4°C overnight, and cerebella cut into thick sections using a rodent brain matrix (Braintree Scientific, Braintree, MA). For each section, the perimeter of both the cerebellum and X-gal-stained region were traced and measured using the ImageJ software package (National Institutes of Health, Bethesda, MD). Section volumes and X-gal stained volumes were determined using areas calculated from the software and known section thickness.

Statistical analyses

Motor scores were analyzed using the Wilcoxon-Mann-Whitney U test or the Kruskal-Wallis test. ANOVA with Bonferroni correction was used for normalized motor scores. Purkinje cell linear densities of normal and *tottering* mice were normally distributed, but Purkinje cell linear densities from mice with Purkinje cell degeneration were not normally distributed. Therefore, all linear density data were analyzed using the Wilcoxon-Mann-Whitney U test, Kruskal-Wallis test or Spearman's rank-order correlation coefficient (r_s). Power analyses (80% power; $\alpha = 0.05$) for Purkinje cell linear densities and EMG RMS amplitude revealed that a sample size of 3 animals was adequate for these experiments. Paired Student's *t* tests were used to compare RMS amplitudes from the EMG. All analyses were performed using the statistical software package Statview (SAS Institute, Cary, NC).

Results

The *Cacna1a* gene, which encodes the α1 subunit of the $Ca_V2.1$ (P/Q-type) calcium channel, was used as a tool to manipulate cerebellar function in the context of dystonic movements. This particular gene is well suited for this strategy as it is abundantly expressed in cerebellum (Tanaka et al., 1995) and there are several engineered mouse strains useful for controlling gene expression. Additionally, numerous mouse strains that carry mutations of *Cacna1a* exhibit generalized dystonia, including the *tottering* mouse mutant (Raike et al., 2005). *Tottering* mice carry a point mutation (Fletcher et al., 1996) that causes episodes of twisting movements and sustained abnormal postures that are best characterized as paroxysmal generalized dystonia based on both clinically defined criteria and EMG (Scholle et al., 2010; Shirley et al., 2008). Although the neuronal pathophysiology underlying the dystonia in *tottering* mice is not yet understood, abnormal cerebellar function is involved. Like some dystonia patients, abnormal cerebellar activation, as determined by c-fos expression, occurs with the dystonia and we have previously demonstrated that cerebellectomy or total elimination of Purkinje cells, the only efferents from cerebellar

cortex, abolishes the dystonia (Campbell et al., 1999; Neychev et al., 2008). While these results suggest that cerebellar signaling is necessary for the expression of dystonia, it was not possible to discern whether the cerebellum actually instigates the dystonia or mediates the severity or anatomical distribution of the dystonia from these all-or-none approaches.

To further explore the relationship between the cerebellum and the involuntary abnormal movements exhibited by these mice, Purkinje cells were gradually eliminated from the *tottering* mouse cerebellum. This was accomplished using the *L7-Sv4* transgene, which causes Purkinje cell death that starts at ∼4 weeks of age and proceeds over the course of several months (Feddersen et al., 1992). The motor phenotype was assessed from 4-25 weeks of age at 3-week intervals in *tottering* mice with progressive Purkinje cell loss (*tottering*$^{PC\text{-}loss}$; Table 1). In *tottering* mice that did not carry the transgene, there was no change with age in the total motor score, which was derived from timed behavioral sampling of abnormal movements of the entire body including head/neck, limbs and trunk (Figure 1A; $p > 0.25$; Kruskal-Wallis test). In contrast, there was a diminution with age in the total motor score of *tottering*$^{PC\text{-}loss}$ mice (Figure 1E; $p < 0.005$; Kruskal-Wallis test). Various body parts were differentially affected. Between 4-7 weeks of age, the motor scores of *tottering* and *tottering*$^{PC\text{-}loss}$ mice were comparable, with no significant difference in the median scores of the limbs, trunk or head/neck between the two groups of mice (Figure 1B-H; $p > 0.05$; Wilcoxon-Mann-Whitney U test). Beginning at 10-13 weeks of age, there was a significant reduction in the motor scores of trunk and head/neck movements ($p < 0.005$ for both regions; Kruskal-Wallis test) but no change in limb movements exhibited by *tottering*$^{PC\text{-}loss}$ mice ($p > 0.1$; Kruskal-Wallis test; Figure 1F-H). Abnormal movements of the head/neck abated by 16-19 weeks of age and abnormal movements of the trunk abated by 22-25 weeks of age, whereas limb movements still were not significantly affected (Figure 1F; $p > 0.1$; Kruskal-Wallis test). All abnormal movements ceased in four *tottering*$^{PC\text{-}loss}$ mice, leaving only a very mild ataxic gait. In contrast, the individual motor scores for limbs, trunk and head/neck region did not change with age in *tottering* mice ($p > 0.5$; Kruskal-Wallis test), consistent with the stability of the total motor scores (Figure 1B-D). These results suggest that as Purkinje cells are lost, the dystonia abates.

The severity of the abnormal movements is related to Purkinje cell density

To determine if the severity of the motor phenotype in *tottering*$^{PC\text{-}loss}$ mice was related to the loss of Purkinje cells, we measured the linear density of Purkinje cells by counting Purkinje cells identified with calbindin. Mice were removed from the study at various time points from 4-25 weeks of age. The linear density of Purkinje cells in *tottering* mice was stable with age (4 week- old = 50.4 PC/mm and 16-19 week-old = 52.7 PC/mm, n = 5-6; $p > 0.5$; Wilcoxon-Mann- Whitney U test). The Purkinje cell linear density in *tottering*$^{PC\text{-}loss}$ mice decreased with age, consistent with previous reports describing similar effects of the *L7-Sv4* transgene (Feddersen etal., 1992). Purkinje cells decreased rapidly in some mice whereas the loss was more protracted in others, which could be attributable to variable transgene expression. As a result, the correlation between age and the linear density of Purkinje cells in *tottering*$^{PC\text{-}loss}$ mice did not reach statistical significance (Figure 2A; $r_s = -0.44$; $p > 0.1$; Spearman's rank-order correlation). However, there was a significant correlation between the motor score and the linear density of Purkinje cells (Figure 2B; $r_s =$

0.82; $p < 0.005$; Spearman's rank-order correlation). These results suggest that the severity of the dystonia in *tottering*$^{PC\text{-}deg}$ mice depended on the density of Purkinje cells.

The density of Purkinje cells determines body parts affected

In *tottering*$^{PC\text{-}loss}$ mice, the abnormal movements and postures subsided in a distinct anatomical pattern, with postures of the head/neck and trunk consistently abating first while abnormal limb movements often persisted. To explore whether this pattern was related to the extent of Purkinje cell loss, *tottering*$^{PC\text{-}loss}$ mice were grouped into three phenotypic categories: 1) generalized dystonic movements, which was defined as abnormal movements in the limbs plus the head/neck and/or trunk, 2) abnormal movements of the limbs only and 3) no abnormal movements. Despite a ∼70% reduction in the median Purkinje cell density compared to *tottering* mice ($p < 0.005$; Wilcoxon-Mann-Whitney U test), *tottering*$^{PC\text{-}loss}$ mice exhibited generalized dystonic movements that were indistinguishable from the generalized dystonic movements of *tottering* mice (Figures 3 and Figure 4A-H). Abnormal movements restricted to the limbs were observed after ∼85% loss of Purkinje cells in *tottering*$^{PC\text{-}loss}$ mice compared to *tottering* mice ($p < 0.005$; Wilcoxon-Mann- Whitney U test). The abnormal movements and postures ceased after ∼90% of the Purkinje cells were eliminated compared to *tottering* mice ($p < 0.005$; Wilcoxon-Mann-Whitney U test), consistent with our previously published results (Campbell et al., 1999; Neychev et al., 2008). The surprising result here was that very few Purkinje cells were required to support generalized dystonic movements and even fewer were necessary to sustain abnormal limb movements.

The distribution of Purkinje cells is not related to the body parts affected

It is possible that the location of the remaining Purkinje cells in *tottering*$^{PC\text{-}loss}$ mice determined the body part(s) affected. Therefore, we examined Purkinje cell loss in *tottering*$^{PC\text{-}loss}$ mice within four cerebellar regions, including the entire vermis, the lateral hemispheres, the anterior lobe (vermis plus hemispheres anterior to the primary fissure) and posterior lobe (vermis plus hemispheres posterior to the primary fissure). Purkinje cell loss in *tottering*$^{PC\text{-}loss}$ mice appeared to be random based on serial cerebellar reconstructions (Figure 4I-L). There was no significant difference in the extent of Purkinje cell loss among any of the cerebellar subregions examined (n = 14 mice; median PC/mm for vermis = 99.6, lateral hemispheres = 86.9, anterior lobe = 106.7, posterior lobe = 81.3; $p = 0.9$; Kruskal-Wallis test). The severity of dystonia in *tottering*$^{PC\text{-}loss}$ mice was correlated with the linear density of Purkinje cells within each subregion examined ($p < 0.05$ for all regions; Spearman's rank-order correlation; not shown), suggesting no obvious correlation between particular regions of the cerebellum and the abnormal movements.

Purkinje cell specific abnormalities evoke abnormal movements

The preceding experiment suggests that cerebellar Purkinje cells are necessary for expression of the dystonia in *tottering* mice. However, it is not clear whether abnormalities restricted to Purkinje cells alone are *sufficient* to generate dystonic movements, since the abnormal *cacna1a* gene is widely expressed in brain. It is possible that Purkinje cells are an essential component of a motor circuit for dystonia but are not responsible for generating the

abnormal movements. We have previously demonstrated that complete elimination of $Ca_V2.1$ channel function specifically within Purkinje cells is sufficient to cause ataxia (Todorov et al., 2011); this was accomplished by breeding the *L7-Cre* transgene, which expresses Cre recombinase in postnatal Purkinje cells, onto the conditional (floxed) *cacna1a* mouse strain (*cacna1a*$^{flox/flox}$). Here, we used a similar strategy to limit a dystonia-causing genetic defect to Purkinje cells. In the homozygous state (*cacna1a*$^{tg/tg}$), the *tottering* mutation results in dystonia associated with a 60% decrement in $Ca_V2.1$ calcium conductance, not complete loss of function (Wakamori et al., 1998). In the heterozygous state, where the *tottering* allele is paired with a normoactive allele (*cacna1a*$^{+/tg}$ or *cacna1a*$^{tg/flox}$), mice do not exhibit abnormal movements (n=8-14, not shown). To isolate a dystonia-causing genotype to Purkinje cells, the *L7-Cre* transgene was bred onto *cacna1a*$^{tg/flox}$ mice, creating mice that expressed only the *tottering* allele in Purkinje cells, but in all other cells, the mice were heterozygous with one normoactive allele and one *tottering* allele (*tottering*$^{PC\text{-}haplo}$ mice). We found that these mice expressed Cre specifically in Purkinje cells (Figure 5A-B). To determine whether abnormalities elsewhere in the brain influence the phenotype, we created mice carrying a *tottering* allele and a knockout (null) allele in all cells (*tottering*^{haplo} mice). Additionally, to control for the effects of Cre recombinase expression within Purkinje cells, the *L7-Cre* transgene was bred onto *tottering* mice *tottering*$^{PC\text{-}Cre}$ mice). Table 1 provides detailed information on all genotypes.

The *tottering*$^{PC\text{-}haplo}$, *tottering*^{haplo} and *tottering*$^{PC\text{-}Cre}$ mutants exhibited widespread abnormal movements (Figure 6A). The motor scores of *tottering* mice and *tottering*$^{PC\text{-}Cre}$ (i.e., *tottering* mice carrying the L7-Cre transgene) mice did not differ, demonstrating that, as expected, expression of Cre recombinase in Purkinje cells had no obvious effect on the severity of the abnormal movements ($p > 0.05$; Wilcoxon-Mann-Whitney U test). However, the motor scores for mice carrying a *tottering* allele and a knockout allele (*tottering*^{haplo}) were significantly worse than *tottering* mice ($p < 0.005$; Wilcoxon-Mann-Whitney U test); this is likely due to a gene dose effect whereby the loss of one *tottering* allele exacerbates the phenotype. The motor scores of the mice in which the *tottering* defect was restricted to Purkinje cells (*tottering*$^{PC\text{-}haplo}$), were also significantly worse than *tottering* mice ($p < 0.0005$; Wilcoxon-Mann-Whitney U test) but were comparable to *tottering*^{haplo} mice (Wilcoxon-Mann-Whitney U test).

To compare the abnormal motor phenotype of *tottering* mice to the *tottering*^{haplo}, *tottering*$^{PC\text{-}haplo}$ and *tottering*$^{PC\text{-}Cre}$ mutants, we assessed the different types of movements and body parts affected. In all genotypes, more than 95% of the abnormal movements were either tonic or clonic (Figure 6B) with no differences among the genotypes ($F_{3, 62} = 2.2$ for tonic and 1.1 for clonic; ANOVA with Bonferroni correction). The anatomical distribution of the abnormal movements was also similar among all four genotypes (Figure 6C), except for a small (5%) but significant shift towards increased head/neck postures in the *tottering*$^{PC\text{-}haplo}$, and *tottering*$^{PC\text{-}haplo}$ mice a ($F_{3, 62} = 6.8$; $p < 0.001$ for *tottering*$^{PC\text{-}haplo}$, ANOVA with Bonferroni correction). Thus, both the appearance of the abnormal movements and the anatomical distribution of the movements in all the novel mouse mutants, including mice in which the dystonia-causing gene defect was restricted to Purkinje cells, were similar to *tottering* mice. From these results we conclude that restricting

dysfunction to Purkinje cells is sufficient to evoke widespread dystonic movements, such as those observed in generalized dystonia.

A small region of cerebellar dysfunction evokes abnormal limb movements

The functional anatomy of the cerebellum is complex. Neighboring microzones corresponding to a single body part can extend across lobules and a single body part can also be represented by multiple non-contiguous microzones (Apps and Garwicz, 2005). Therefore, it is not clear that a small region of cerebellar dysfunction could cause abnormal movements in a single part of the body, such as those observed in focal dystonia.

To determine if a small region of cerebellar dysfunction could cause abnormal postures of an isolated body region, we refined the conditional genetic approach used in the previous experiment to perturb only a fraction of the cerebellum. To do this, lentivirus-encoding Cre recombinase was injected directly into the cerebella of *Cacna1a*$^{tg/flox}$ mice, creating a small region of Cre-positive cells leading to a small region of cerebellum with the *tottering*^{haplo} genotype (Figure 5C-D). To control for the nonspecific effects of the viral injection, another group of *Cacna1a*$^{tg/flox}$ mice was injected with the same lentivirus vector that encoded green fluorescent protein (GFP) instead of Cre recombinase, creating a small region of GFP-positive cells. For these experiments, our goal was to affect only 10-15% of the cerebellum based on the results of the *tottering*$^{PC\text{-}loss}$ experiments, which suggested that ∼10-15% of Purkinje cells was adequate to sustain isolated abnormal movements. The *Rosa26* Cre reporter locus, which is permissive for β-galactosidase expression in the presence of Cre recombinase, was used to estimate the cerebellar volume affected by Cre recombinase after lentivirus injection. X-gal staining revealed that the Cre lentiviral injections affected 10±2% of the entire cerebellum (Figure 7; 7.1±1.6 mm^3 of the 69.3±2.8 mm^3 cerebellum, n = 5); similar volumes were observed in the mice injected with the control GFP lentivirus (not shown).

Mice injected with the Cre lentivirus into either midline or lateral cerebellum exhibited significantly more abnormal movements than control mice injected with GFP lentivirus (Figure 8A; $p < 0.01$; Wilcoxon-Mann-Whitney U test). Both midline and lateral cerebellar injections produced comparable patterns of movement. Most (66%) of the abnormal movements were isolated to a single body part, such as the hindlimb (Figure 8C-D). The hindlimb was most commonly affected by tonic flexion or extension, accounting for 90% of the abnormal movements. Clonic movements of the head/neck (8%) or tonic flexion or extension of the trunk (2%) were less frequent.

To determine if regionally restricted motor abnormalities evoked with Cre lentivirus could be produced with an alternative independent method, we applied direct electrical stimulation to the cerebellum in awake and unrestrained mice. Previous studies have shown that stimulation amplitudes of 100-400 μA affects ∼0.03-24.43 mm^3 of brain tissue (Ranck, 1975), which is ∼0.05-35.4% of the mouse cerebellum. We therefore examined the motor consequences of cerebellar stimulation with 100- 400 μA. Although it is a formal possibility that antidromic stimulation could activate cerebellar afferents, others, using similar stimulation parameters to map deep cerebellar nuclei, have ruled out such effects (Cicirata et

al., 1992). Prior to stimulation, abnormal motor behavior was not observed (n = 14; Figure 8B). Stimulation with 100 μA pulses did not induce abnormal movements (n = 13; Wilcoxon-Mann-Whitney U test). In contrast, 200 μA pulses evoked obvious abnormal movements (n = 8-14; $p < 0.01$ for all; Wilcoxon-Mann-Whitney U test). These abnormal movements were even more obvious at 300-400 μA, with a greater number of body parts affected (n = 8-14; $p < 0.01$ for all; Wilcoxon- Mann-Whitney U test). Based on the median number of body parts affected, 200 μA pulses typically affected only a single body part, whereas 300 or 400 μA pulses affected more regions. Abnormal movements occurred mainly in the limbs (85%), and sometimes occurred in the head/neck (14%) or trunk (1%), especially at higher amplitudes. The abnormal limb movements were predominantly tonic (84%), while clonic movements (7%) and tremor (9%) were infrequently observed (Figure 8C). Abnormal movements always occurred ipsilateral to the stimulation site. No histological signs of cell death were found postmortem (not shown) suggesting that the abnormal movements were caused by dysfunction rather than destruction of cerebellar tissue.

To better understand whether the isolated abnormal limb movements induced by a small region of cerebellar dysfunction resembled the movements typical of generalized dystonia in *tottering* mice, EMG was used to record activity from the hindlimb muscles, tibialis (TA) and gastrocnemius (GS) in awake freely moving mice. During normal walking, low amplitude TA and GS muscle activation was observed in control mice (not shown), *tottering* mice (Figure 9A) and $Cacna1a^{tg/flox}$ mice treated with Cre lentivirus (Figure 9B). There were no significant differences in the amplitudes of TA or GS EMG activity between the three groups of mice during walking (Table 2). Consistent with a previous study (Scholle et al., 2010), abnormal hindlimb movements exhibited by *tottering* mice with generalized dystonia were associated with significant increases in the amplitude of the EMG in both TA and GS (Figure 9A; Table 2). Significant increases in EMG amplitude, which were comparable to the increases observed in *tottering* mice, were also associated with the isolated abnormal hindlimb movements in $Cacna1a^{tg/flox}$ mice treated with Cre lentivirus (Figure 9B; Table 2). In contrast, normal mice did not exhibit increases in EMG amplitude even after vigorous movement of the hindlimb such as scratching (Table 2). These results suggest that the abnormal movements that occurred only in the hindlimb of $Cacna1a^{tg/flox}$ mice treated with Cre lentivirus have EMG characteristics of dystonia.

Discussion

Here, we demonstrated that a small region of cerebellar dysfunction induced isolated abnormal movements. Only 10-15% of the normal number of Purkinje cells was required for abnormal movements that were restricted to the limbs in *tottering* mice. Lentiviral-mediated conditional genetic disruptions of ∼10% of the cerebellum induced isolated abnormal movements. Focused electrical stimulation of the cerebellum also caused isolated abnormal movements ipsilateral to the site of stimulation, consistent with the ipsilateral connectivity of the cerebellum. Thus, a variety of perturbations that affected only 10-15% of the cerebellum resulted in isolated abnormal movements. The isolated movements were generally tonic movements of one hindlimb, regardless of the type of insult. EMG recorded during isolated abnormal hindlimb movements was indistinguishable from the hindlimb

EMG recorded during generalized dystonia in *tottering* mice indicating that the isolated abnormal movements were comparable to dystonic movements. Overall these results suggest that a small region of cerebellar dysfunction is sufficient to generate motor abnormalities that are best described as focal dystonia.

Restricting a dystonia-causing genotype to Purkinje cells in the *tottering*$^{PC\text{-}haplo}$ mice resulted in a movement disorder that was somewhat more severe but otherwise comparable to the generalized dystonic movements exhibited by *tottering* mice in terms of the type of movements and body parts affected. The *tottering*$^{PC\text{-}haplo}$ mice carried a *tottering* allele and a null allele within Purkinje cells, and all other cells were heterozygous with one normoactive allele and one *tottering* allele. Therefore, it is possible that, in addition to Purkinje cells, other heterozygous brain regions of the *tottering*$^{PC\text{-}haplo}$ mice contributed to the phenotype, although mice that are heterozygous for the *tottering* allele do not typically exhibit any obvious abnormal phenotype. A role for other brain regions in the abnormal movements seems unlikely in light of the motor phenotype exhibited by *tottering*$^{PC\text{-}haplo}$ mice. In contrast to the *tottering*$^{PC\text{-}haplo}$ mice, the *tottering*^{haplo} mice carried a *tottering* allele and a null allele throughout the CNS, not just Purkinje cells. If other brain regions contributed to the dystonic phenotype, we would have expected more severe or different types of movements in the *tottering*^{haplo} mice compared to *tottering*$^{PC\text{-}haplo}$. However, by all measures, the abnormal movements exhibited by *tottering*^{haplo} and *tottering*$^{PC\text{-}haplo}$ mice were indistinguishable. These results suggest that defects of a single cell type, Purkinje cells, are sufficient to instigate dystonia.

We exploited several different genetic tools in mice to demonstrate that similar pathomechanisms may govern both focal and generalized dystonia by adjusting the extent of the same underlying *Cacna1a* gene defect. *CACNA1A* gene defects in humans were first associated with episodic ataxia type 2, familial hemiplegic migraine, or spinocerebellar ataxia type 6; focal and segmental dystonia is increasingly recognized as a salient feature of these disorders (Arpa et al., 1999; Cuenca-Leon et al., 2009; Jen et al., 2007). Additionally, some patients with *CACNA1A* mutations exhibit only dystonia (Cuenca-Leon et al., 2009; Giffin et al., 2002; Roubertie et al., 2008; Sethi and Jankovic, 2002; Spacey et al., 2005). Despite this association, these mutations are rare and account for only a very small fraction of dystonia patients, so it is possible that the motor abnormalities produced by the *Cacna1a* defects reflect a gene-specific pathology that is not shared by other dystonias. However, focal dystonia was also produced in normal mice using low amplitude electrical stimulation of the cerebellum and we have previously demonstrated that AMPA receptor activation in cerebellum of normal mice instigates generalized dystonia (Fan et al., 2012; Pizoli et al., 2002). These results argue that abnormal cerebellar signaling may be a common pathway for inducing both focal and generalized dystonia, regardless of whether the abnormality arises from genetic, physiological or pharmacological influences. Thus, while *Cacna1a* mutations are rare, it is reasonable to infer broader applicability for the concept presented here that, in some instances, different forms of dystonia likely reflect a gradient of cerebellar dysfunction.

Abnormal movements were most frequently induced in the hindlimb. Both vermal and lateral cerebellar injections of lentivirus produced abnormal limb movements. Further, after

widespread Purkinje cell loss in *tottering* mice, abnormal limb movements persisted and were associated with few remaining Purkinje cells scattered throughout the cerebellum. The propensity for focal dystonia of the hindlimb in mice may arise from the disproportionate representation of the hindlimbs in rodent cerebellum rather than the precise location of the insult. In rodents, hindlimbs are represented by more than half of Purkinje cell climbing fiber responses in the vermal and intermediate zones of cerebellar lobules II to VI, whereas the face and trunk are each represented by only ∼10% of responses (Logan and Robertson, 1986). However, in humans, focal dystonias most commonly occur in the neck, hand and face (Defazio et al., 2004). Consistent with these clinical observations, and in contrast to rodent, neck, hand and face are more frequently represented in the primate cerebellum than the leg (Robertson and Laxer, 1981), which may, in part, account for the distribution of focal dystonias in humans.

Animal models are useful for generating mechanistic explanations for phenomena observed in patients. Such hypotheses can then be tested in humans to promote our understanding of the disease process. Although an increase in cerebellar metabolic activity is consistently observed in humans in many different types of focal dystonia (Galardi et al., 1996; Hutchinson et al., 2000; Odergren et al., 1998; Preibisch et al., 2001) and many different types of generalized dystonia (Argyelan et al., 2009; Ceballos-Baumann et al., 1995; Eidelberg et al., 1998; Kluge et al., 1998), it is not clear whether a common cerebellar pathomechanism could underlie both types of dystonia. The work presented here in animals suggests the cerebellum has the capacity to instigate both focal and generalized dystonic movements. However, this does not exclude the possibility that different pathomechanisms play a role in other types of focal dystonia. For example, it has been suggested that focal dystonias associated with overuse, such as musicians dystonia, may arise from enlarged or displace somatotopic representations in the cortex (Bara-Jimenez et al., 1998; Delmaire et al., 2005; Thickbroom et al., 2003). These results are important for all focal dystonias because they demonstrate that a few dysfunctional neurons can cause focal dystonia. Abnormalities within such a small population may go undetected even with the most advanced neuroimaging techniques. Further, understanding whether different forms of dystonia share common pathological substrates has implications for treatment. The results presented here suggest that some focal and generalized dystonias may be treated with similar therapeutic strategies.

Acknowledgments

This work was supported by United States National Institutes of Health (R01 NS33592, R01 NS40470 and the Emory Core Facilities grant, P30 NS055077), the Dystonia Medical Research Foundation and Tyler's Hope for a Dystonia Cure Foundation. We thank Luis E. Soria-Jasso, Cecilia Prudente, Ryan Kuhar, Megan E. Bailey, Meyeon Shin and Molly E. Ogle for technical assistance, Dr. Kerry Ressler for the lentivirus constructs, Dr. Rodney Feddersen for the *L7-Sv4* transgenic mice and Dr. David Yue for *Cacanla*$^{+/-}$ mice.

References

Apps R, Garwicz M. Anatomical and physiological foundations of cerebellar information processing. Nat Rev Neurosci. 2005; 6:297–311. [PubMed: 15803161]

Argyelan M, Carbon M, Niethammer M, Ulug AM, Voss HU, Bressman SB, Dhawan V, Eidelberg D. Cerebellothalamocortical connectivity regulates penetrance in dystonia. J Neurosci. 2009; 29:9740–7. [PubMed: 19657027]

Arpa J, Cuesta A, Cruz-Martinez A, Santiago S, Sarria J, Palau F. Clinical features and genetic analysis of a Spanish family with spinocerebellar ataxia 6. Acta Neurol Scand. 1999; 99:43–47. [PubMed: 9925237]

Bara-Jimenez W, Catalan MJ, Hallett M, Gerloff C. Abnormal somatosensory homunculus in dystonia of the hand. Ann Neurol. 1998; 44:828–31. [PubMed: 9818942]

Bressman SB, Raymond D, Fuchs T, Heiman GA, Ozelius LJ, Saunders-Pullman R. Mutations in THAP1 (DYT6) in early-onset dystonia: a genetic screening study. Lancet Neurol. 2009; 8:441–6. [PubMed: 19345147]

Brown LL, Lorden JF. Regional cerebral glucose utilization reveals widespread abnormalities in the motor system of the rat mutant dystonic. J Neurosci. 1989; 9:4033–41. [PubMed: 2585066]

Calderon DP, Fremont R, Kraenzlin F, Khodakhah K. The neural substrates of rapid-onset Dystonia Parkinsonism. Nat Neurosci. 2011; 14:357–65. [PubMed: 21297628]

Camargos S, Scholz S, Simon-Sanchez J, Paisan-Ruiz C, Lewis P, Hernandez D, Ding J, Gibbs JR, Cookson MR, Bras J, Guerreiro R, Oliveira CR, Lees A, Hardy J, Cardoso F, Singleton AB. DYT16, a novel young-onset dystonia-parkinsonism disorder: identification of a segregating mutation in the stress-response protein PRKRA. Lancet Neurol. 2008; 7:207–15. [PubMed: 18243799]

Campbell DB, Hess EJ. Cerebellar circuitry is activated during convulsive episodes in the tottering (tg/tg) mutant mouse. Neuroscience. 1998; 85:773–83. [PubMed: 9639271]

Campbell DB, North JB, Hess EJ. Tottering mouse motor dysfunction is abolished on the Purkinje cell degeneration (pcd) mutant background. Exp Neurol. 1999; 160:268–278. [PubMed: 10630211]

Ceballos-Baumann AO, Passingham RE, Marsden CD, Brooks DJ. Motor reorganization in acquired hemidystonia. Ann Neurol. 1995; 37:746–757. [PubMed: 7778848]

Cicirata F, Angaut P, Serapide MF, Panto MR, Nicotra G. Multiple representation in the nucleus lateralis of the cerebellum: an electrophysiologic study in the rat. Exp Brain Res. 1992; 89:352–62. [PubMed: 1623979]

Cuenca-Leon E, Banchs I, Serra SA, Latorre P, Fernandez-Castillo N, Corominas R, Valverde MA, Volpini V, Fernandez-Fernandez JM, Macaya A, Cormand B. Late- onset episodic ataxia type 2 associated with a novel loss-of-function mutation in the CACNA1A gene. J Neurol Sci. 2009; 280:10–4. [PubMed: 19232643]

Defazio G, Abbruzzese G, Livrea P, Berardelli A. Epidemiology of primary dystonia. Lancet Neurol. 2004; 3:673–8. [PubMed: 15488460]

Delmaire C, Krainik A, Tezenas du Montcel S, Gerardin E, Meunier S, Mangin JF, Sangla S, Garnero L, Vidailhet M, Lehericy S. Disorganized somatotopy in the putamen of patients with focal hand dystonia. Neurology. 2005; 64:1391–6. [PubMed: 15851729]

Devanagondi R, Egami K, LeDoux MS, Hess EJ, Jinnah HA. Neuroanatomical substrates for paroxysmal dyskinesia in lethargic mice. Neurobiol Dis. 2007; 27:249–57. [PubMed: 17561408]

Eidelberg D, Moeller JR, Antonini A, Kazumata K, Nakamura T, Dhawan V, Spetsieris P, deLeon D, Bressman SB, Fahn S. Functional brain networks in DYT1 dystonia. Ann Neurol. 1998; 44:303–312. [PubMed: 9749595]

Fan X, Hughes KE, Jinnah HA, Hess EJ. Selective and sustained AMPA receptor activation in cerebellum induces dystonia in mice. J Pharmacol Exp Ther. 2012; 340:733–741. [PubMed: 22171094]

Feddersen RM, Ehlenfeldt M, Yunis WS, Clark HB, Orr HT. Disrupted cerebellar cortical development and progressive degeneration of Purkinje cells in SV40 T antigen transgenic mice. Neuron. 1992; 9:955–966. [PubMed: 1419002]

Fletcher CF, Lutz CM, O'Sullivan TN, Shaughnessy JD, Hawkes R, Frankel WN, Copeland NG, Jenkins NA. Absence epilepsy in tottering mutant mice is associated with calcium channel defects. Cell. 1996; 87:607–617. [PubMed: 8929530]

Fureman BE, Jinnah HA, Hess EJ. Triggers of paroxysmal dyskinesia in the calcium channel mouse mutant tottering. Pharmacol Biochem Behav. 2002; 73:631–637. [PubMed: 12151038]

Galardi G, Perani D, Grassi F, Bressi S, Amadio S, Antoni M, Comi GC, Canal N, Fazio F. Basal ganglia and thalamo-cortical hypermetabolism in patients with spasmodic torticollis. Acta Neurol Scand. 1996; 94:172–176. [PubMed: 8899050]

Giffin NJ, Benton S, Goadsby PJ. Benign paroxysmal torticollis of infancy: four new cases and linkage to CACNA1A mutation. Dev Med Child Neurol. 2002; 44:490–493. [PubMed: 12162387]

Hadj-Sahraoui N, Frederic F, Zanjani H, Herrup K, Delhaye-Bouchaud N, Mariani J. Purkinje cell loss in heterozygous staggerer mutant mice during aging. Brain Res Dev Brain Res. 1997; 98:1–8.

Heckroth JA, Goldowitz D, Eisenman LM. Purkinje cell reduction in the reeler mutant mouse: a quantitative immunohistochemical study. J Comp Neurol. 1989; 279:546–55. [PubMed: 2918086]

Hutchinson M, Nakamura T, Moeller JR, Antonini A, Belakhlef A, Dhawan V, Eidelberg D. The metabolic topography of essential blepharospasm. Neurology. 2000; 55:673–677. [PubMed: 10980732]

Jen JC, Graves TD, Hess EJ, Hanna MG, Griggs RC, Baloh RW. Primary episodic ataxias: diagnosis, pathogenesis and treatment. Brain. 2007; 130:2484–93. [PubMed: 17575281]

Kamm C. Early onset torsion dystonia (Oppenheim's dystonia). Orphanet J Rare Dis. 2006; 1:48. [PubMed: 17129379]

Kluge A, Kettner B, Zschenderlein R, Sandrock D, Munz DL, Hesse S, Meierkord H. Changes in perfusion pattern using ECD-SPECT indicate frontal lobe and cerebellar involvement in exercise-induced paroxysmal dystonia. Mov Disord. 1998; 13:125–134. [PubMed: 9452337]

LeDoux MS, Lorden JF, Ervin J. Cerebellectomy eliminates the motor syndrome of the genetically dystonic rat. Exp Neurol. 1993; 120:302–310. [PubMed: 8491286]

Logan K, Robertson LT. Somatosensory representation of the cerebellar climbing fiber system in the rat. Brain Res. 1986; 372:290–300. [PubMed: 3708365]

Maguschak KA, Ressler KJ. Beta-catenin is required for memory consolidation. Nat Neurosci. 2008; 11:1319–26. [PubMed: 18820693]

Nemeth AH. The genetics of primary dystonias and related disorders. Brain. 2002; 125:695–721. [PubMed: 11912106]

Neychev VK, Fan X, Mitev VI, Hess EJ, Jinnah HA. The basal ganglia and cerebellum interact in the expression of dystonic movement. Brain. 2008; 131:2499–509. [PubMed: 18669484]

Neychev VK, Gross RE, Lehericy S, Hess EJ, Jinnah HA. The functional neuroanatomy of dystonia. Neurobiol Dis. 2011; 42:185–201. [PubMed: 21303695]

Odergren T, Stone-Elander S, Ingvar M. Cerebral and cerebellar activation in correlation to the action-induced dystonia in writer's cramp. Mov Disord. 1998; 13:497–508. [PubMed: 9613744]

Pizoli CE, Jinnah HA, Billingsley ML, Hess EJ. Abnormal cerebellar signaling induces dystonia in mice. J Neurosci. 2002; 22:7825–7833. [PubMed: 12196606]

Preibisch C, Berg D, Hofmann E, Solymosi L, Naumann M. Cerebral activation patterns in patients with writer's cramp: a functional magnetic resonance imaging study. J Neurol. 2001; 248:10–17. [PubMed: 11266013]

Raike RS, Jinnah HA, Hess EJ. Animal models of generalized dystonia. NeuroRx. 2005; 2:504–12. [PubMed: 16389314]

Ranck JB Jr. Which elements are excited in electrical stimulation of mammalian central nervous system: a review. Brain Res. 1975; 98:417–40. [PubMed: 1102064]

Robertson LT, Laxer KD. Localization of cutaneously elicited climbing fiber responses in lobule V of the monkey cerebellum. Brain Behav Evol. 1981; 18:157–68. [PubMed: 7248741]

Roubertie A, Echenne B, Leydet J, Soete S, Krams B, Rivier F, Riant F, Tournier-Lasserve E. Benign paroxysmal tonic upgaze, benign paroxysmal torticollis, episodic ataxia and CACNA1A mutation in a family. J Neurol. 2008; 255:1600–2. [PubMed: 18758887]

Scholle HC, Jinnah HA, Arnold D, Biedermann FH, Faenger B, Grassme R, Hess EJ, Schumann NP. Kinematic and electromyographic tools for characterizing movement disorders in mice. Mov Disord. 2010; 25:265–74. [PubMed: 20077474]

Sethi KD, Jankovic J. Dystonia in spinocerebellar ataxia type 6. Mov Disord. 2002; 17:150–3. [PubMed: 11835453]

Shirley TL, Rao LM, Hess EJ, Jinnah HA. Paroxysmal dyskinesias in mice. Mov Disord. 2008; 23:259–64. [PubMed: 17999434]

Spacey SD, Materek LA, Szczygielski BI, Bird TD. Two novel CACNA1A gene mutations associated with episodic ataxia type 2 and interictal dystonia. Arch Neurol. 2005; 62:314–6. [PubMed: 15710862]

Tanaka O, Sakagami J, Kondo H. Localization of mRNAs of voltage-dependent Ca2+- channels: four subtypes of a1 and b-subunits in developing and mature rat brain. Brain Res Mol Brain Res. 1995; 30:1–16. [PubMed: 7609630]

Thickbroom GW, Byrnes ML, Stell R, Mastaglia FL. Reversible reorganisation of the motor cortical representation of the hand in cervical dystonia. Mov Disord. 2003; 18:395–402. [PubMed: 12671945]

Todorov B, Kros L, Shyti R, Plak P, Haasdijk ED, Raike RS, Frants RR, Hess EJ, Hoebeek FE, De Zeeuw CI, van den Maagdenberg AM. Purkinje Cell-Specific Ablation of Ca(V)2.1 Channels is Sufficient to Cause Cerebellar Ataxia in Mice. Cerebellum. 2011 Epub ahead of print.

Todorov B, van de Ven RC, Kaja S, Broos LA, Verbeek SJ, Plomp JJ, Ferrari MD, Frants RR, van den Maagdenberg AM. Conditional inactivation of the Cacna1a gene in transgenic mice. Genesis. 2006; 44:589–94. [PubMed: 17146767]

Ulug AM, Vo A, Argyelan M, Tanabe L, Schiffer WK, Dewey S, Dauer WT, Eidelberg D. Cerebellothalamocortical pathway abnormalities in torsinA DYT1 knock-in mice. Proc Natl Acad Sci U S A. 2011; 108:6638–43. [PubMed: 21464304]

Wakamori M, Yamazaki K, Matsunodaira H. Single tottering mutations responsible for the neuropathic phenotype of the P-type calcium channel. J Biol Chem. 1998; 52:34857–34867. [PubMed: 9857013]

Zhao Y, Sharma N, LeDoux MS. The DYT1 carrier state increases energy demand in the olivocerebellar network. Neuroscience. 2011; 177:183–94. [PubMed: 21241782]

Zoons E, Booij J, Nederveen AJ, Dijk JM, Tijssen MA. Structural, functional and molecular imaging of the brain in primary focal dystonia--a review. Neuroimage. 2011; 56:1011–20. [PubMed: 21349339]

Highlights

- the extent of cerebellar dysfunction determines the extent of dystonic movements
- small regions of cerebellar dysfunction produced movements resembling focal dystonia
- focal and generalized dystonias may arise through similar mechanisms
- Purkinje cells mediate dystonia

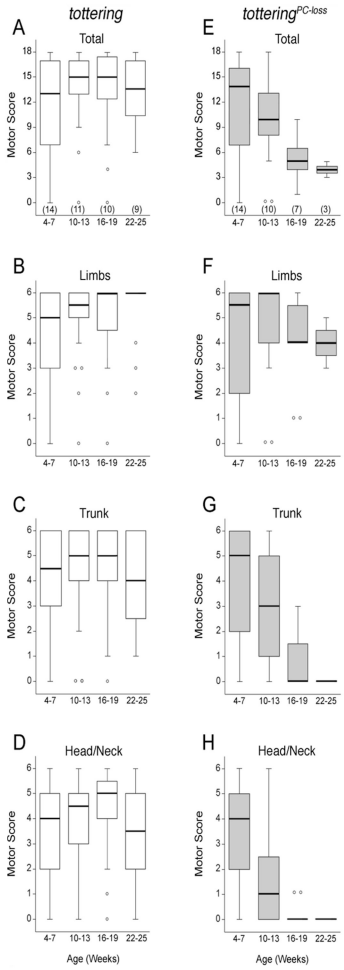

Figure 1. Anatomical distribution and severity of dystonia as a function of age in and *tottering* and *tottering*$^{PC\text{-}loss}$ mice

In *tottering*$^{PC\text{-}loss}$ mice, the *L7-Sv4* transgene (*L7-Sv4*) was used to gradually eliminate Purkinje cells from the cerebellum. T*ottering* mouse (white boxes) and *tottering*$^{PC\text{-}loss}$ (gray boxes) data are expressed in box and whisker format with outliers represented by open circles. Sample sizes are in parentheses. In *tottering* mice the (**A**) total motor score and individual motor scores for postures of the (**B**) limbs, (**C**) trunk and (**D**) head/neck region did not significantly change with age. In *tottering*$^{PC\text{-}loss}$ mice, the motor score for the (**F**) limbs did not change significantly with age, whereas the (**E**) total motor score and scores for the (**G**) trunk and (**H**) head/neck region significantly decreased with age.

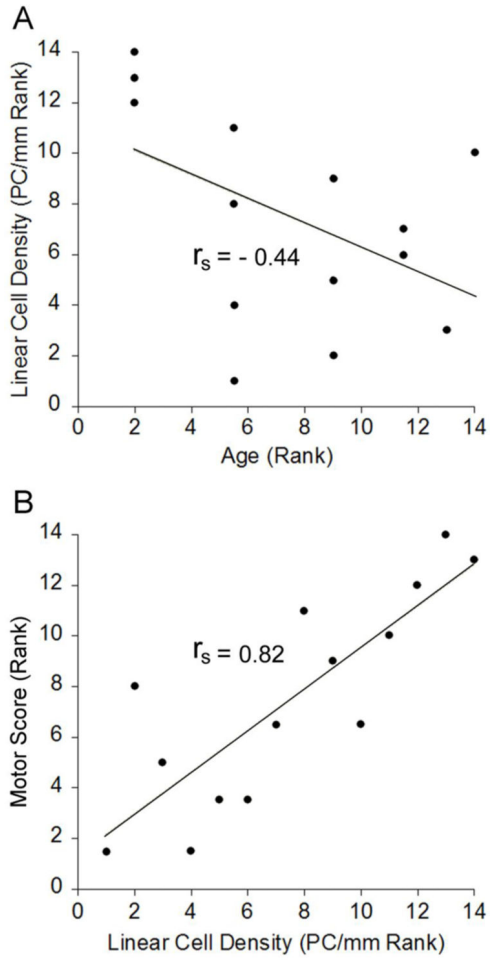

Figure 2. Correlation between motor score and Purkinje cell density in *tottering*$^{PC\text{-}loss}$ mice

Data (n =14) were analyzed using the Spearman's rank-order correlation coefficient (r_s). (**A**) There was no significant correlation between linear density of Purkinje cells and age in *tottering*$^{PC\text{-}loss}$ mice. (**B**) There was a significant correlation between total motor score and the linear density of Purkinje cells in *tottering*$^{PC\text{-}loss}$ mice.

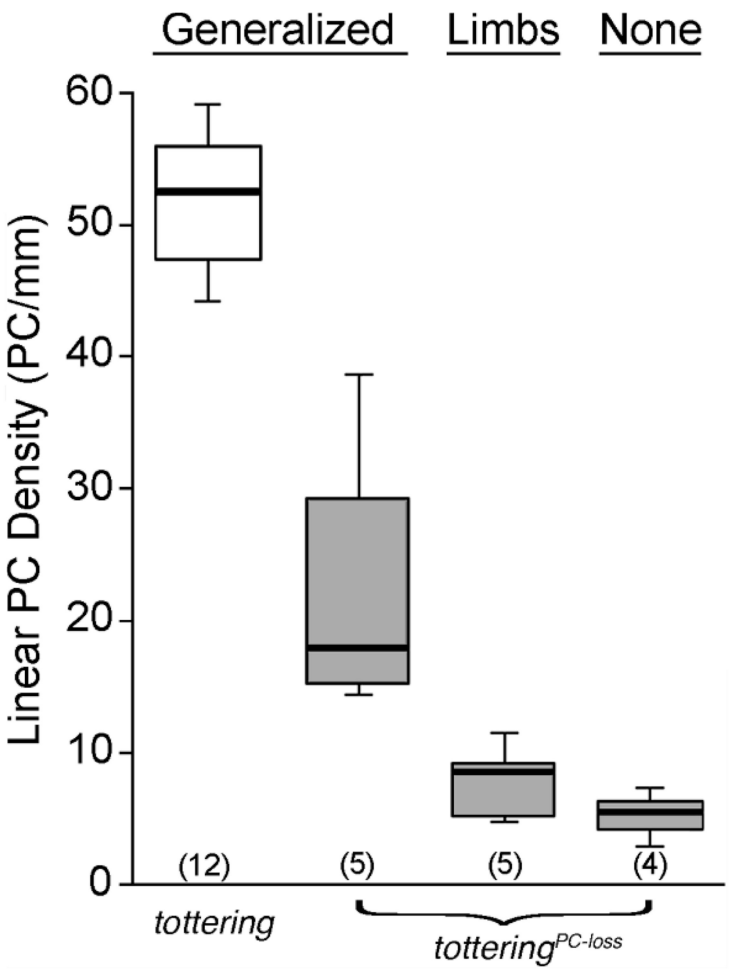

Figure 3. Distribution of abnormal movements relative to Purkinje cell density in *tottering*$^{PC\text{-}loss}$ mice

Tottering$^{PC\text{-}loss}$ mice (i.e., *tottering* mice carrying the *L7-Sv4* transgene) were grouped into three phenotypic categories, including generalized dystonic movements, dystonic movements of the limbs only or no abnormal movements. The linear density of Purkinje cells was determined for *tottering*$^{PC\text{-}loss}$ mice (gray boxes) and for normal *tottering* littermates that did not carry the *L7-Sv4* transgene (white box). Data are expressed in box and whisker format and samples sizes are in parentheses.

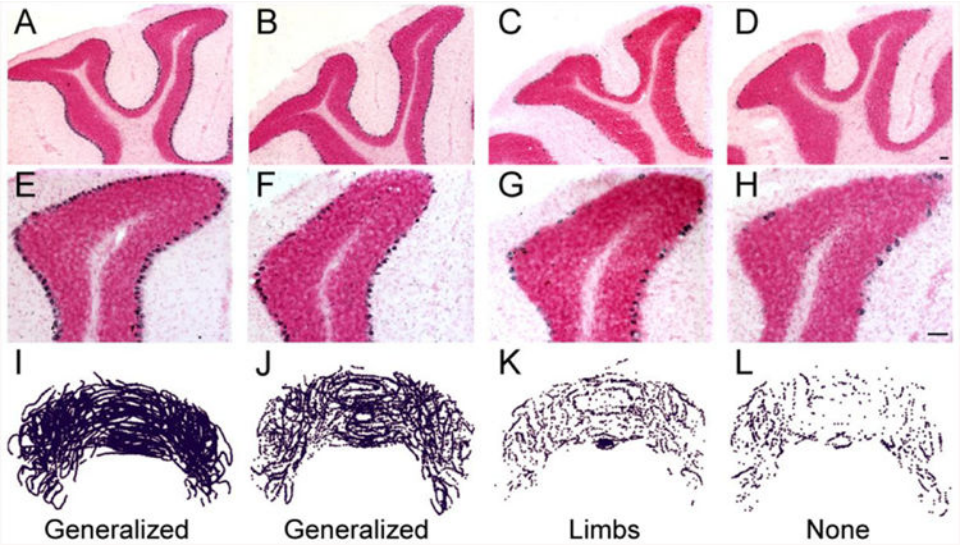

Figure 4. *In situ* hybridization for calbindin mRNA in cerebellar sections from *tottering* and *tottering*$^{PC\text{-}loss}$ mice

(**A**-**H**) Cerebellar sections from *tottering* and *tottering*$^{PC\text{-}loss}$ mice were hybridized with a cRNA probe for calbindin labeled with digoxigenin (purple) and counterstained with Nuclear Fast Red. (**A** and **E**) Compared to sections from their *tottering* littermates without Purkinje cell loss, (**B** and **F**) sections from *tottering*$^{PC\text{-}loss}$ mice with generalized dystonia exhibited an obvious loss of cerebellar Purkinje cells. (**C** and **G**) The loss was more advanced in *tottering*$^{PC\text{-}loss}$ mice with focal dystonia. (**D**, **H**) Few Purkinje cells remained *tottering*$^{PC\text{-}loss}$ in mice in which dystonia completely abated. Serial reconstructions of cerebellar sections from (**I**) *tottering* mice and *tottering*$^{PC\text{-}loss}$ mice with (**J**) generalized, (**K**) focal and (**L**) no dystonia demonstrate the apparent uniform distribution of the *L7-Sv4*-induced Purkinje cell degeneration. Scale bars = 100 μm.

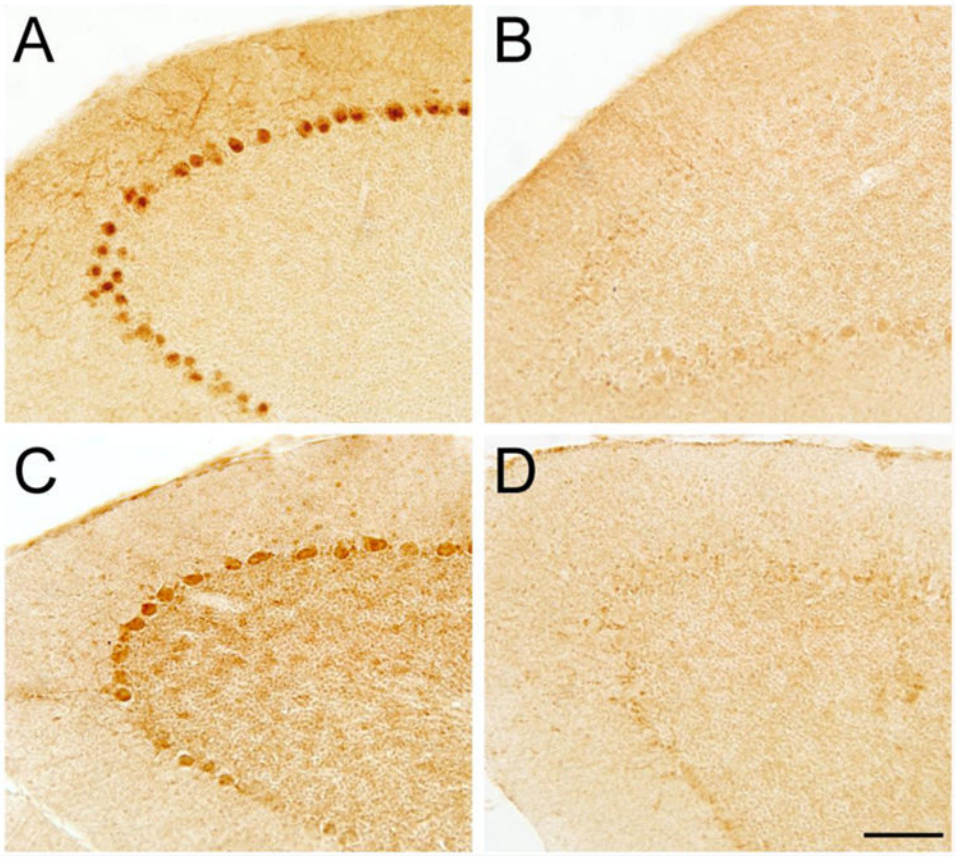

Figure 5. Induction of β-galactosidase expression in the cerebellum by Cre recombinase

(**A**) Purkinje cell-specific staining was observed in *tottering*$^{PC\text{-}loss}$ (*Cacna1a*$^{tg/flox}$ mice carrying the Purkinje cell specific *L7-Cre* transgene) that also carried the *Rosa26* Cre reporter allele. There was no obvious Purkinje cell loss in these mice. (**B**) No staining was observed in *Cacna1a*$^{tg/flox}$ mice carrying the *Rosa26* Cre reporter allele but not the *L7-Cre* transgene. (**C**) *Cacna1a*$^{tg/flox}$ mice carrying the *Rosa26* Cre reporter allele treated with intracerebellar injections of Cre-lentivirus revealed induction of β-galactosidase expression near the injection site. (**D**) Staining was absent in sections distant from the Cre-lentivirus injection site. Scale bar = 100 μm.

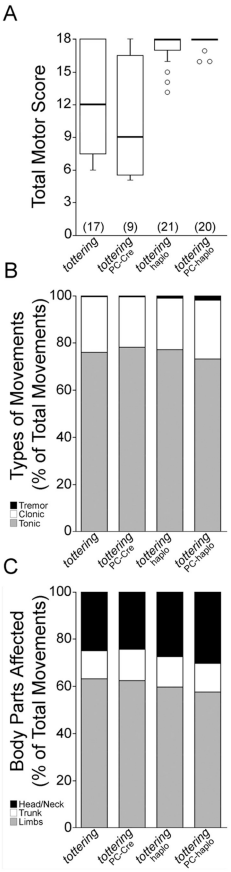

Figure 6. Abnormal cerebellar Purkinje cells evoke abnormal movements

(**A**) The motor scores of *tottering* and *tottering*$^{PC\text{-}cre}$ mice were not significantly different, whereas the scores of *tottering*$^{PC\text{-}haplo}$ and *tottering*^{haplo} mice were significantly greater than *tottering* mice. Motor scores are expressed in box and whisker format and sample sizes are in parentheses. (**B**) The types of movements exhibited by all four genotypes were similar and no significant differences were noted for tonic or clonic movements. (**C**) The anatomical distribution of the abnormal movements was similar across all four genotypes, but *tottering*$^{PC\text{-}haplo}$ and *tottering*^{haplo} mice exhibited a slight increase in head/neck and decrease in limb postures. Abnormal movement type and anatomical distribution data are expressed as percentage of total movements.

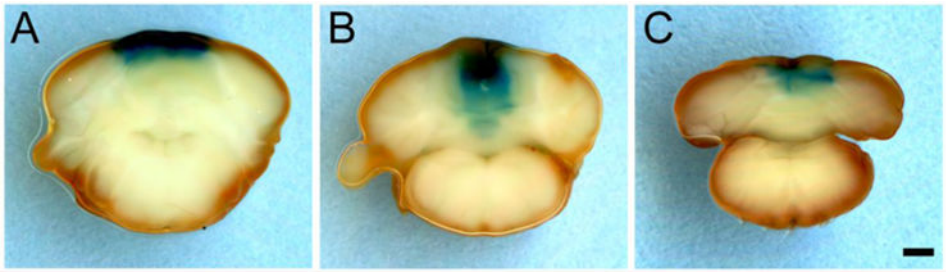

Figure 7. β-galactosidase expression induced by intracerebellar injections of Cre recombinase lentivirus

To determine the volume of cerebellum affected by injections of lentivirus expressing Cre recombinase, whole-mount X-gal staining was performed in tissue from *Cacna1a*$^{tg/flox}$ carrying the *Rosa26* Cre-reporter. (**A**-**C**) Representative staining observed in sections from three different mice near the injection site. Scale bar = 1 mm.

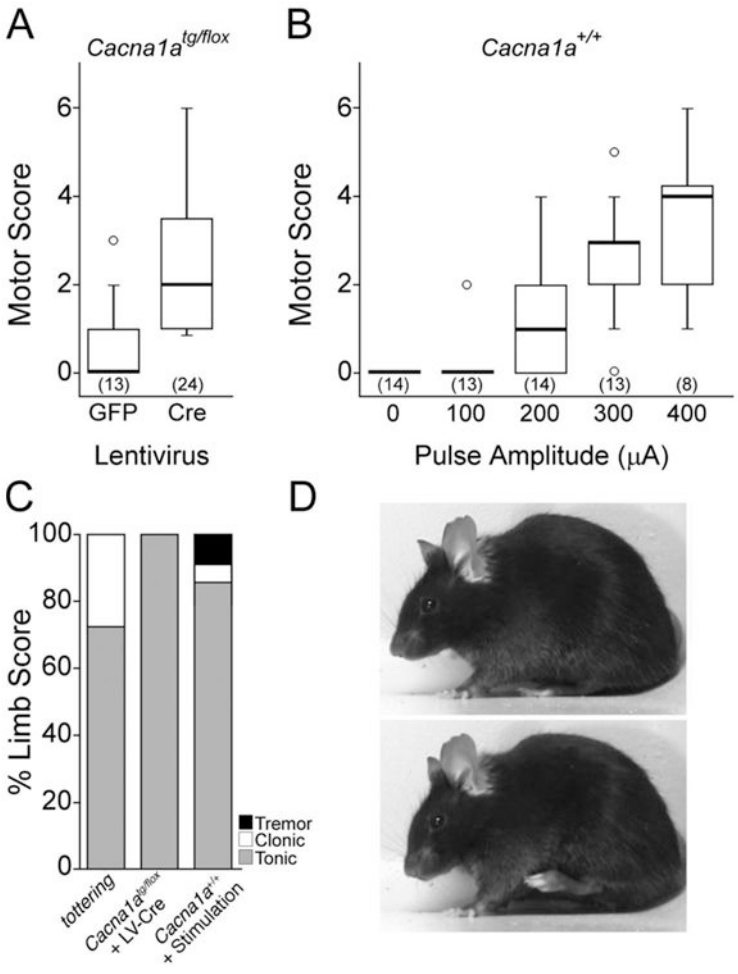

Figure 8. A small region of cerebellar dysfunction evokes isolated abnormal movements

(**A**) Cre recombinase lentivirus was injected into the cerebella of *Cacna1a*$^{tg/flox}$ mice (Cre) to generate a small region of abnormal cerebellum. GFP lentivirus was injected into the cerebellum of other *Cacna1a*$^{tg/flox}$ mice (GFP) as a control. The GFP lentivirus caused no abnormal movements, while the Cre lentivirus induced focal motor abnormalities. Motor scores are expressed in box and whisker format and sample sizes are in parentheses. (**B**) Cerebellar stimulation in awake, freely-moving normal mice. Pulse amplitudes of 200-400 μA induced motor abnormalities. Motor scores are expressed in box and whisker format and sample sizes are in parentheses. (**C**) Abnormal hindlimb movements in *tottering* mice, *Cacna1a*$^{tg/flox}$ mice treated with intracerebellar lentivirus expressing Cre recombinase (*Cacna1a*$^{tg/flox}$ + LV-Cre) and electrically-stimulated normal mice (*Cacna1a*$^{+/+}$ + Stimulation) were predominantly hypertonic. The types of movements are expressed as percentage of total limb movements. (**D**) An example of the abnormal hindlimb flexion movements typically observed in the Cre-treated *Cacna1a*$^{tg/flox}$ mice, which exhibited a normal baseline (top), but often exhibited abnormal hindlimb flexion movements (bottom).

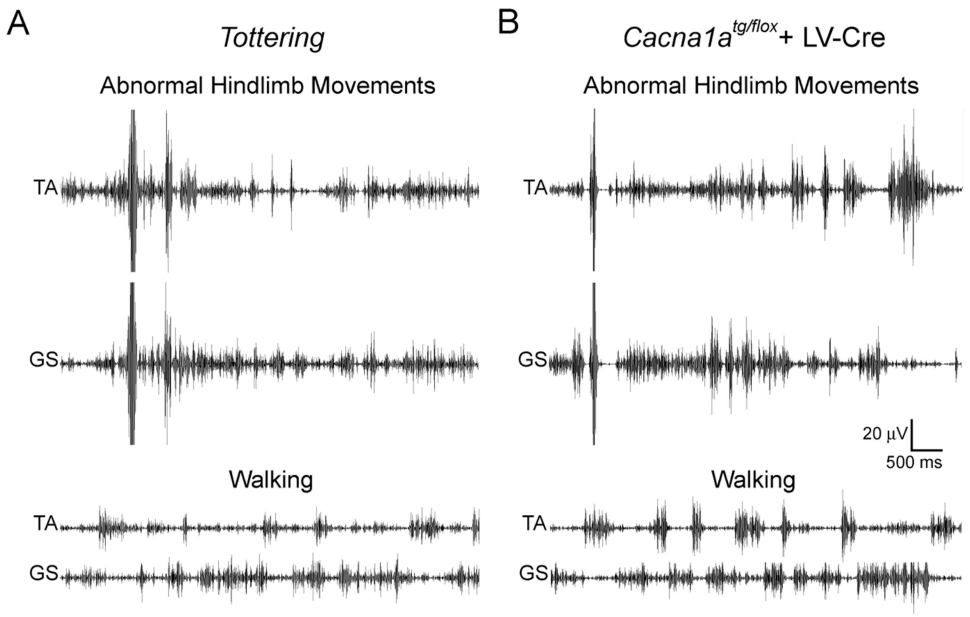

Figure 9. Abnormal hindlimb movements are associated with muscle overactivation

EMG was recorded from the hindlimb muscles, tibialis (TA) and gastrocnemius (GS), in awake, freely- moving **(A)** *tottering* mice and **(B)** *Cacna1a*$^{tg/flox}$ mice treated with Cre-lentivirus (+ LV-Cre) during normal walking (lower traces) and with abnormal movements (upper traces).

Table 1
Experimental and control mice used for the study

Common Name	Genotype	Description	Motor Phenotype
Normal	*Cacna1a*$^{+/+}$	Normal C57BL/6J mice	Normal
Tottering	*Cacna1a*$^{tg/tg}$	Two *tottering* alleles throughout	Dystonic
Tottering$^{PC\text{-}loss}$	*Cacna1a*$^{tg/tg}$; *L7-SV4*$^{+/-}$	*Tottering* mice with gradual Purkinje cell loss	Gradually diminishing dystonia
Heterozygous *tottering*	*Cacna1a*$^{+/tg}$	One *tottering* and one normal allele throughout	Normal
Heterozygous *tottering*-floxed	*Cacna1a*$^{tg/flox}$	One *tottering* and one normal “floxed” allele	Normal
Tottering$^{PC\text{-}Cre}$	*Cacna1a*$^{tg/t}$; *L7-Cre*$^{+/-}$	*Tottering* mice expressing Cre recombinase in Purkinje cells	Dystonic
Tottering^{haplo}	*Cacna1a*$^{tg/-}$	One *tottering* and one null allele throughout	Dystonic
Tottering$^{PC\text{-}haplo}$	*Cacna1a*$^{tg/flox}$; *L7-Cre*$^{+/-}$	One *tottering* and one null allele in Purkinje cells, but otherwise one and one *tottering* normal “floxed” allele throughout	Dystonic

Table 2

Peak EMG amplitudes in hindlimb with normal movements and abnormal postures

	Walking		Scratching	
	TA(μV)	GS(μV)	TA(μV)	GS(μV)
Normal control; n=3	9±1	16±1	10±2	17±2
	Walking		Abnormal postures	
	TA(μV)	GS(μV)	TA(μV)	GS(μV)
Tottering; n=5	10±3	16±3	22±8*	29±6*
Cacna1a$^{tg/flox;}$ + LV-Cre; n=4	12±1	18±1	20±2*	27±2**

Data expressed as mean peak RMS amplitude ± SEM and analyzed with paired Student's *t* test;

* $p < 0.05$,

** $p < 0.01$.